Available online at www.sciencedirect.com
ScienceDirect
Nuclear Instruments and Methods in Physics Research B 259 (2007) 7–13
NIM B
Beam Interactions with Materials & Atoms
www.elsevier.com/locate/nimb

# MICADAS: A new compact radiocarbon AMS system

Hans-Arno Synal [a,*], Martin Stocker [b], Martin Suter [b]

[a] Paul Scherrer Institute, c/o ETH Hönggerberg, Building HPK, CH-8093 Zürich, Switzerland
[b] Particle Physics, ETH Hönggerberg, Building HPK, CH-8093 Zürich, Switzerland

Available online 25 January 2007

**Abstract**

A novel tabletop AMS system with overall dimensions of only $2.5 \times 3\ m^2$ has been built and tested. The mini radiocarbon dating System (MICADAS) is based on a vacuum insulated acceleration unit that uses a commercially available 200 kV power supply to generate acceleration fields in a tandem configuration. At the high-energy end, ions in charge state $1^+$ are selected and interfering molecules of mass 14 amu are destroyed in multiple collisions. The new system is now fully operational. It is the prototype of a new generation of radiocarbon spectrometers which fulfill the requirements for radiocarbon dating applications as well as for the less demanding $^{14}C/^{12}C$ isotopic ratio measurements as needed, e.g. in biomedical applications. A detailed description of the system is given and results of performance tests are discussed.


*PACS:* 01.50.Pa; 82.80.Ms; 41.75.−I; 41.85.−p; 41.90.+e; 42.15.Eq; 0.7.75.+h

*Keywords:* Accelerator mass spectrometry; Tabletop AMS spectrometer; Vacuum insulated high voltage device; Radiocarbon dating

## 1. Introduction

In the recent past, impressive progress has been made to simplify the AMS measurement technique and to provide easier-to-operate instruments and high-performance commercial AMS spectrometers to the AMS user community. However, the ultimate goal of having AMS instrumentation with tabletop dimensions and a system complexity and costs similar to those of conventional mass spectrometers has not yet been reached. To take a next step forward, we have focused on pushing the AMS technique, in particular that of radiocarbon, towards lower beam energies. The destruction of molecular interferences using multiple ion gas collisions has resulted in acceleration systems which operate in the 500 kV range which gives the maximum of yield for $1^+$ radiocarbon ions [1]. It has been demonstrated that this method can be applied at even lower energies [2], with an important consequence. At acceleration voltages of less than approximately 200 kV, a new design for the acceleration stage of an AMS spectrometer is possible. This provides the opportunity to build a new, more compact generation of AMS spectrometers.

## 2. System description

The design concept of the new instrument follows ideas developed for AMS spectrometers using the $1^+$ charge state, which utilize multiple collisions to dissociate molecular interferences. This technique has been shown to eliminate background from interfering molecules to levels where radiocarbon dating of natural samples becomes possible [1]. The MICADAS spectrometer is a very compact instrument of $2.5 \times 3\ m^2$ overall dimensions, as shown in Fig. 1. The novel feature of this instrument is the acceleration unit. In contrast to other AMS spectrometers which use conventional particle accelerators, a vacuum insulated high voltage platform is utilized to generate energetic ions. Neither a pressure vessel to insulate the high voltage terminal nor acceleration tubes are needed for beam transport. The overall dimensions of the acceleration unit are $1.1 \times 0.6\ m^2$. It has been tested in combination with the

* Corresponding author. Tel.: +41 1 633 2027; fax: +41 1 633 1067.
*E-mail address:* synal@phys.ethz.ch (H.-A. Synal).

0168-583X/$ - see front matter © 2007 Elsevier B.V. All rights reserved.
doi:10.1016/j.nimb.2007.01.138

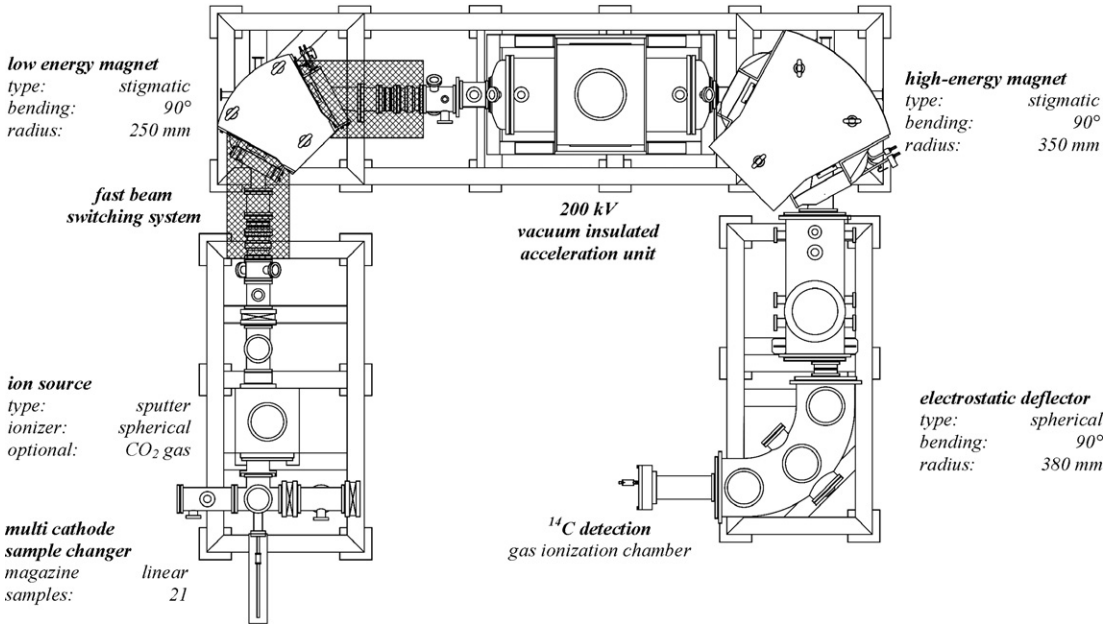


Fig. 1. The layout of MICADAS. The system design avoids open high voltage potentials. All necessary power supplies are integrated into the support stands of the instrument and do not require additional laboratory space. Operation procedures, in particular sample and magazine exchanges can be carried out without interrupting the measurement process. With its small dimensions of $2.5 \times 3\ m^2$ it can be easily fit into a common laboratory environment.

mass spectrometers of our 500 kV Pelletron AMS system [2]. Based on the results, we have designed and constructed a dedicated radiocarbon AMS spectrometer. Details of its primary components are given below.

### 2.1. The ion source

In combination with the new AMS spectrometer, we also decided to build a new ion source. While there are commercial high current sputter ion sources available which are suitable for high-performance radiocarbon measurements, the design of those sources would have set too many limitations to reaching our goal of a tabletop system with no open high voltage potentials. First, we wanted to have an ion source with a vacuum box at ground potential. Thus, all operations at the source, e.g. exchange of sample magazines, could be made without interrupting source operation. We therefore designed the source such that all high voltages are fed into the vacuum chamber from below. A high voltage deck is integrated into the support stand of the source, hosting the power supplies required for Cs beam generation and negative ion extraction. The design allows extraction energies of up to 40 keV. A spherical ionizer is used to produce the sputtering $Cs^+$ beam. The cesium reservoir is located inside the ion source box. The sputter energy can be chosen between 5 and 12 keV. Two lenses are used to focus the cesium beam onto the sputter target. A turbo molecular pump with 500 l/s pumping speed is attached to the ion source box. Under normal operation conditions, the residual gas pressure is a few times $10^{-7}$ hPa. Typical negative ion currents are 30–50 μA for processed graphite targets. Higher currents have been achieved by increasing Cs flow, but have not yet been utilized for measurements. The source is equipped with a multi-cathode sample changer. We use a linear 21-position magazine which is located outside the ion source box in a separate vacuum chamber. A mechanism can transfer the different cathodes holding the sample material into the sputtering position inside the ion source. Exchange of a cathode takes between 10–20 s depending on the position in the magazine. Magazines can be exchanged via a vacuum lock within 15–20 min. One single cathode can be measured during magazine changes.

In addition to graphite targets, gaseous $CO_2$ samples can be directly analyzed with this source. A mixture of He and $CO_2$ can be fed into the sputter region. A capillary is used to maintain the pressure gradient between source vacuum and gas feed system. Ti cones are used as a catalyst and $^{12}C^-$currents of up to 10 μA have been extracted. At present, gas operation is at an experimental stage. In the future, we plan a direct coupling with an elemental analyzer to analyze samples of small sizes (<50 μg).

### 2.2. Low energy mass spectrometer

At the low energy side, a dipole magnet (bending radius 25 cm) is used for mass analysis. It is designed to accept ion beams of about $10\pi$ mm mrad $\sqrt{\text{MeV}}$ emmittance, which is a typical value for the cesium sputter ion source in use. At the focal points before and after the magnet, variable slit apertures are installed. At the magnet image plane, an offset Faraday cup is placed to measure the negative ion current extracted from the ion source. This makes it possible

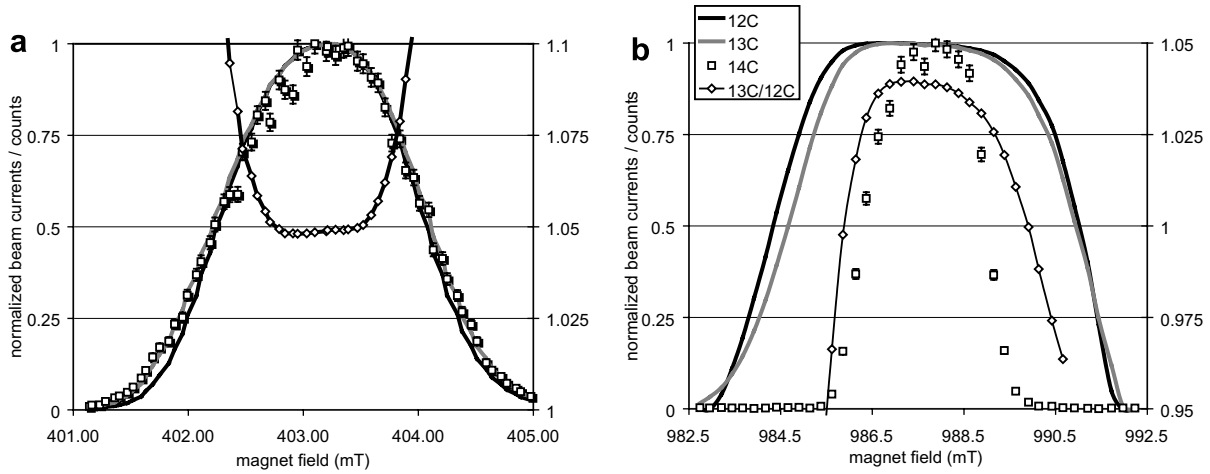


Fig. 2. Beam scans, performed with the low energy magnet and the high-energy magnet of the system, are shown in (a) and (b), respectively. Measurements of the stable isotope currents were made with the Faraday cups located at the focal plane of the high-energy magnet. The radiocarbon ions were measured after the ESA using our gas ionization detector. In both cases, a nice flat top situation is observed for the $^{13}C/^{12}C$ isotope ratios.

to monitor the transmission through the acceleration unit. The injection spectrometer is equipped with a fast beam pulsing system that enables injection of beams into the acceleration unit in very short pulses [3]. The time structure for the different isotope beams is 50 μs, 40 ms, 500 μs and 40 ms for $^{12}C$, $^{14}C$, $^{13}C$ and $^{14}C$, respectively. For measurement, the beam pulses of the different isotopes are matched carefully as shown in Fig. 2(a). This plot shows the beam currents of the different carbon isotopes, measured at the high-energy end of the system, which are plotted as function of the magnetic field of the injection magnet. Because of the small stripper diameter, a flat top situation cannot be achieved completely. However, over a quite wide range of magnet field intensity, very stable $^{13}C/^{12}C$ and $^{14}C/^{12}C$ isotopic ratios are observed. This is a precondition for high quality isotopic ratio measurements.

### 2.3. The acceleration unit

To accelerate the ions, a high voltage platform inside a vacuum chamber is used. Two gap lenses maintain the voltage gradient between terminal and ground potential in a tandem configuration. The entrance and the exit of the platform are formed as electrodes of these gap lenses. Their counterparts are mounted on the entrance and exit flanges of the vacuum vessel, respectively. They can be aligned mechanically to the potential electrodes in order to minimized aberrations due to geometric imperfection of the lens assemblies. The high voltage is generated with a commercially available HV power supply (Heinzinger Type: PNC 200,000-5) connected to the platform via a high voltage vacuum feedthrough, providing the terminal voltage of up to 200 kV. At the HV platform, the charge exchange canal is located inside a differentially pumped housing. Three turbo molecular pumps (mounted at ground potential) are used to remove the stripper gas. We use $N_2$ as stripper gas. At a stripper pressure high enough to get rid of any molecular interference, a residual gas pressure of less than $10^{-6}$ hPa can be maintained in the vacuum system of the acceleration unit. Gas is fed into the stripper canal from outside the vacuum via a high-pressure gas transfer line. An all-metal leak valve operated by a rotating shaft is used to regulate the gas flow to obtain the proper density of stripper gas.

### 2.4. High-energy mass spectrometer

Ions emerging from the acceleration unit are analyzed in an achromatic mass spectrometer. First, a stigmatic 90° magnet with 35 cm mean bending radius performs $p/q$ separation. At the focal plane of this magnet, Faraday cups are placed to measure the beam currents of the stable carbon isotopes $^{12}C$ and $^{13}C$. A third cup is used to measure the current of $^{13}C$ molecular fragments which result from $^{13}CH^-$ molecules. These molecules are injected together with $^{14}C$, but will break up in the stripper, and the $^{13}C^+$ fragments can be measured as an ion current. The position of this beam is between the $^{12}C$ and $^{13}C$ beams. This is a good parameter to use for background corrections. The Faraday cups have wide openings and a nice flat top of the measured beam currents as well as of the obtained $^{13}C/^{12}C$ isotope ratio is achieved (Fig. 2(b)).

A spherical electrostatic analyzer follows this magnet. It has a bending radius of 38 cm, a gap of 3 cm, and together with the magnet it provides non-energy dispersive beam transport. An aperture slit can be placed at the beam waist of the magnet to limit the energy acceptance of the spectrometer. Under normal operation conditions, a total beam transmission of about 40% is achieved. If we assume a 50% yield of charge state $1^+$ ions [4], a total ion optical transmission of 80% can be calculated. This is in good agreement with our design values which were based on angular straggling calculations using the Sigmund Winterbon formalism [5].

### 2.5. Detection system

To complete the spectrometer, a gas ionization chamber is used to identify the $^{14}C$ ions. The detector window is a $5 \times 5$ mm $Si_3N_{3.1}$ [6] foil of thickness 50 nm, and the detector gas is *iso*butane at a pressure of about 20 hPa. Ions are stopped within the first 5 cm of the active detector volume and dissipate a total energy of 428 keV. The total energy signal is used for particle identification. With the present setup, we achieve a FWHM of the $^{14}C$ peak that corresponds to relative energy resolution of 7.7%. In the future, we will use cooled FET pre-amplifiers reduce the electronic noise component. In combination with a smaller detector capacitance, a relative energy resolution of 5–6% can be expected. In addition, we plan a $\Delta E/E_{res}$ measurement to improve separation capability, and thus reduce background from molecular fragments reaching the final detector.

## 3. Measurements and performance tests

### 3.1. Background

If ions in the $1^+$ charge state are used, interfering molecules have to be destroyed in multiple collisions with stripper gas atoms/molecules. The fragmentation of mass 14 molecules is shown in Fig. 3 as a function of residual gas pressure as measured inside the vacuum vessel of the acceleration unit. This parameter was used as a proxy for the stripper density. The events detected with the final gas ionization chamber are normalized to the current measured with the high-energy $^{12}C$ Faraday cup. With increasing pressure, an exponential reduction of molecules reaching the final detector is observed. Extrapolating this curve to the stripper density used in dating measurements, allows estimation of the background from undestroyed molecules. Under these conditions, this background component would correspond to a $^{14}C/^{12}C$ isotopic ratio well below $10^{-16}$. However, there are other ions reaching the final detection system. This background component comes from $^{13}C$ molecular fragments which leave the stripper as $2^+$ ions and react in the acceleration section in a $2^+ \rightarrow 1^+$ charge changing collision. If this happens at certain point in the acceleration section, the $^{13}C$ ions will have the same $p/q$ ratio as the $^{14}C$ and can traverse the magnet on the mean path trajectory. Even though they have the wrong $E/q$ ratio, a second scattering event will allow a fraction of these ions to reach the detector.

Measurements of different blank samples with quite a large range of $^{13}CH^-$ beam impurities show a nice correlation between measured $^{13}C(H)$ currents and observed ions in the detection system (see Fig. 4). In order to test the hypothesis that these ions are $^{13}C$ molecular fragments, we introduced additional gas into the high-energy acceleration section via a needle valve, increasing the gas density in the critical part of the acceleration section where $2^+ \rightarrow 1^+$ charge-changing collisions are expected. We observed a linear correlation of the number of the detected ions with respect to the residual gas density in the acceleration sections, as would be expected if background arises from $^{13}CH$ fragments.

To test the system detection limit, blank samples produced from unprocessed graphite powder have been analyzed. Typically, they give isotopic ratios below $2 \times 10^{-15}$, which corresponds to ages of about 50 kyrs. For blank

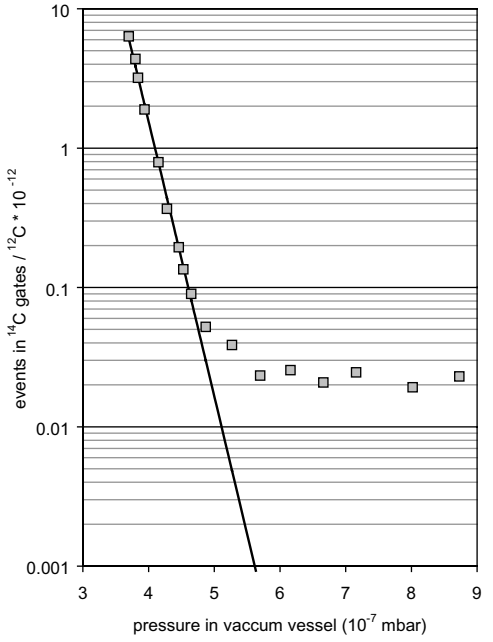


Fig. 3. Molecular dissociation is shown as function of stripper density. As this configuration does not allow a direct measurement of the stripper gas density, the residual gas pressure in the vacuum vessel is used as a proxy. Radiocarbon measurements are performed at $6.5–7 \times 10^{-7}$ hPa. Here, any remaining mass 14 molecules are well below the level of $10^{-16}$.

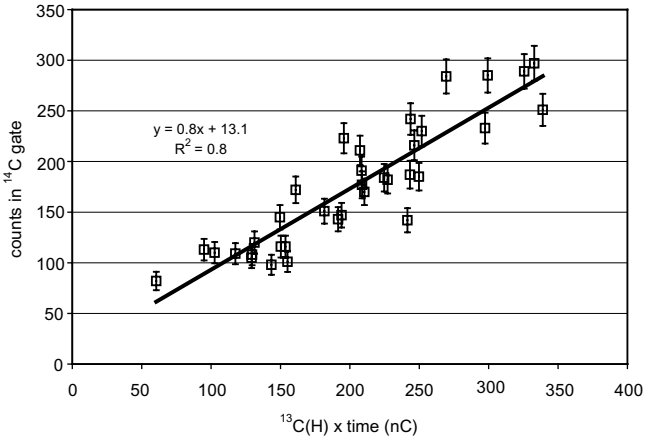


Fig. 4. For all analyzed blank samples, the number of ions detected in the $^{14}C$ gates are plotted as function of total charge of $^{13}C$ molecular fragments, which has been measured with the $^{13}C(H)$ Faraday cup after the high-energy magnet. The obvious correlation indicates a background component proportional to molecular impurities in the mass 14 beam. This correlation is utilized to apply a background correction.

samples processed in our graphitization line, we observe $^{14}C/^{12}C$ ratios between $4 \times 10^{-15}$ and $15 \times 10^{-15}$ depending on the actual content of $^{13}CH$ molecules in the extracted ion beam. We have also analyzed blank samples which have been processed using Mn to reduce $CO_2$ to graphite [7]. These samples have very little $^{13}CH$ content. Consequently, we observed $^{14}C/^{12}C$ ratios similar to those from the unprocessed graphite powder.

### 3.2. Performance tests

First performance tests of the system were made with samples of the radiocarbon standard material Oxalic Acid I. The results of measurements of five replicate cathodes made from this material are shown in Fig. 5(a) and (b) for the $^{14}C/^{12}C$ and $^{13}C/^{12}C$ ratios, respectively. Each sample was analyzed in 6–7 runs of 200 s measurement time each and a typical counting statistics-based uncertainty of 0.3% was reached (internal uncertainty). The external estimates of the uncertainty of mean values of the different samples correspond nicely to their internal counting statistics-based uncertainties. The average of the mean values of the different samples is in excellent agreement with the total mean value of all independent measurements. The whole data set is statistically consistent at an uncertainty of better than 2‰. In addition to the radiocarbon ratios, $\delta^{13}C$ values are measured directly with the instrument. The reproducibility of the measurements for individual cathodes varies between 0.3‰ and 0.7‰. Using the average value of all standards for normalization, we get deviations of the individual cathodes from the nominal value of the standard material of less than 0.6‰. This shows the high quality of the stable isotope ratio measurements.

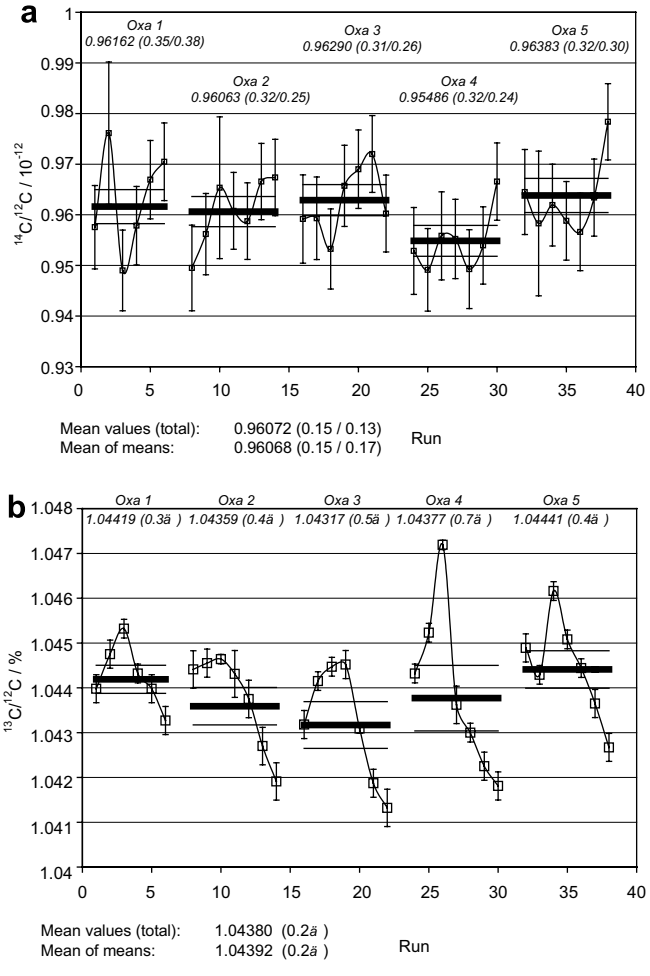


Fig. 5. $^{14}C/^{12}C$, $^{13}C/^{12}C$ isotopic ratios measured for a set of 5 Oxalic Acid I standards. The different standards have been analyzed in a preprogrammed sequence, one after the other, to a total of six to seven runs. The scatter of the $^{14}C/^{12}C$ ratios is dominated by the counting statistics of the individual measurements. The average values are shown in the plot for the different standards. In the following brackets, the internal uncertainty due to counting statistics and the external uncertainty of the mean value are given, respectively. The more precise $^{13}C/^{12}C$ ratios reveal a trend with respect to the duration of the measurement. Only the external uncertainties of the mean values are given in case of the $^{13}C/^{12}C$ ratios.

To test the dating capability of the MICADAS instrument, a dedicated trial with FIRI [8] samples D, F, H, I, J has been conducted. From materials D and F, four independent samples were produced in our graphitization line. Three graphite samples were made from materials H and I and two from material J. All 16 samples were of approximately 1 mg of carbon. Each sample was divided into three sub-samples, of which two were pressed into individual cathodes to perform two independent measurements of the same material. The third part of the different samples of the same material were mixed and 4, 4, 2, 2 and 2 individual cathodes were pressed from the mixtures of materials D, F, H, I and J, respectively. The total set of 46 samples was distributed into three magazines each with 20 positions. Within each magazine two individually processed blank samples and three oxalic acid I standards were included.

Measurements of the three magazines were performed unattended following a preprogrammed sequence in which all samples of a magazine were analyzed in eight runs. Every run of a single cathode was subdivided into 10 cycles of 20 s each. Thus, a total of about 27 min of measurement time was spent on each cathode. The negative $^{12}C$ ion currents of the various samples were about 30 μA. For a standard sample, typically 130,000 $^{14}C$ counts was detected. The $^{14}C/^{12}C$ isotope ratios measured for the processed blank samples ranged from $5 \times 10^{-15}$ to $16 \times 10^{-15}$ and a clear correlation to the measured currents of the $^{13}C$ molecular fragments was observed. This is shown in Fig. 4, where events detected in the $^{14}C$ window are plotted as function of the product of the measured $^{13}C(H)$ current and the measurement time. The obvious correlation makes us confident to apply a background correction using the slope of the correlation function. After background correction, blanks gave $^{14}C/^{12}C$ ratios of about $4 \times 10^{-15}$, which is very similar to values observed for the same material using our EN-Tandem $^{14}C$ spectrometer.

Normalization of isotope ratios has been made run-wise using the average value of the three independent standard measurements for both $^{14}C/^{12}C$ ratios and $\delta^{13}C$ values.

Results are compiled in Table 1. All in all, there is a good agreement between our measurements and the published consensus values of the different materials. The results of the measurements of the 31 single cathodes prepared from the different samples show a very consistent picture. At a precision level of 37 yrs (average uncertainty of samples based on counting statistics, standard normalization, background, and blank correction), the reduced $\chi^2$-value of 0.98 indicates no randomly distributed external uncertainty component. For the 15 different samples which were produced in the same graphitization process, we can average the two independent measurements. Thus, we reach a precision level of 26 yrs and a reduced $\chi^2$-value of 1.1. Again, this is a good indication that there is no significant external uncertainty component. The situation changes if we average over all cathodes prepared from the same material. The reduced $\chi^2$-value of 3.6 shows that at a counting precision of about 15 yrs, a significant variation is present among samples of the same materials, but from different preparation processes. Two arguments suggest that these differences do not come from the measurement process itself. First, the measured $\delta^{13}C$ values agree within a fraction of a per mill between independent measurements of the same graphite material, but can show differences of up to several per mill for different graphitizations. Second, the results for the mixtures we prepared from all graphite

Table 1
Compilation of results from the dedicated performance test with FIRI samples D, F, H, I, and J

| Cathode label | $\delta^{13}C$‰ | $^{14}C$ Age yr BP | Error ± yr | $\sigma$ ± yr | $\chi^2$ | Graphite label | $^{14}C$ Age yr BP | Error ± yr | $\sigma$ ± yr | $\chi^2$ | Cons. value |
|---|---|---|---|---|---|---|---|---|---|---|---|
| FD11 | −24.8 | 4577 | 37 | 36 | 0.95 | FD1 | 4542 | 26 | 35 | 1.79 | |
| FD12 | −24.6 | 4507 | 37 | 23 | 0.40 | | | | | | |
| FD21 | −25.5 | 4489 | 38 | 27 | 0.52 | FD2 | 4488 | 28 | 1 | 0.00 | |
| FD22 | −25.8 | 4487 | 40 | 47 | 1.36 | | | | | | |
| FD31 | −24.8 | 4520 | 38 | 44 | 1.35 | FD3 | 4526 | 28 | 6 | 0.05 | |
| FD32 | −25.2 | 4532 | 40 | 32 | 0.65 | | | | | | |
| FD41 | −24.2 | 4549 | 37 | 51 | 1.87 | | | | | | |
| **FD** | **−25.0** | **4523** | **14** | **12** | **0.73** | | | | | | **4508** |
| FD-mix | −24.3 | 4576 | 20 | 15 | 0.56 | | | | | | **−24.8** |
| FF11 | −23.3 | 4533 | 36 | 44 | 1.51 | FF1 | 4512 | 26 | 21 | 0.65 | |
| FF12 | −23.8 | 4491 | 38 | 43 | 1.30 | | | | | | |
| FF21 | −23.4 | 4505 | 37 | 28 | 0.58 | FF2 | 4489 | 27 | 17 | 0.39 | |
| FF22 | −22.5 | 4472 | 38 | 39 | 1.03 | | | | | | |
| FF31 | −22.8 | 4562 | 36 | 24 | 0.45 | FF3 | 4539 | 26 | 23 | 0.79 | |
| FF32 | −23.5 | 4516 | 37 | 25 | 0.45 | | | | | | |
| FF41 | −25.8 | 4398 | 39 | 30 | 0.58 | FF4 | 4396 | 27 | 2 | 0.01 | |
| FF42 | −26.2 | 4394 | 38 | 24 | 0.40 | | | | | | |
| **FF** | **−23.9** | **4484** | **13** | **21** | **2.63** | | | | | | **4508** |
| FF-mix | −24.2 | 4503 | 19 | 11 | 0.36 | | | | | | **−24.8** |
| FH11 | −26.8 | 2161 | 37 | 29 | 0.61 | FH1 | 2207 | 25 | 46 | 3.20 | |
| FH12 | −25.6 | 2252 | 35 | 27 | 0.57 | | | | | | |
| FH21 | −26.5 | 2143 | 37 | 31 | 0.68 | FH2 | 2161 | 26 | 18 | 0.47 | |
| FH22 | −26.4 | 2179 | 37 | 39 | 1.13 | | | | | | |
| FH31 | −22.2 | 2223 | 34 | 18 | 0.30 | FH3 | 2254 | 24 | 31 | 1.61 | |
| FH32 | −21.7 | 2284 | 34 | 18 | 0.27 | | | | | | |
| **FH** | **−24.9** | **2207** | **15** | **23** | **2.40** | | | | | | **2232** |
| FH-mix | −22.7 | 2237 | 17 | 11 | 0.41 | | | | | | **−25.0** |
| FI11 | −24.0 | 4406 | 40 | 63 | 2.45 | FI1 | 4417 | 28 | 11 | 0.14 | |
| FI12 | −23.4 | 4427 | 40 | 46 | 1.31 | | | | | | |
| FI21 | −25.2 | 4346 | 40 | 35 | 0.75 | FI2 | 4401 | 29 | 55 | 3.69 | |
| FI22 | −25.0 | 4456 | 41 | 40 | 0.96 | | | | | | |
| FI31 | −20.3 | 4623 | 39 | 36 | 0.86 | FI3 | 4588 | 28 | 36 | 1.66 | |
| FI32 | −19.9 | 4552 | 39 | 31 | 0.61 | | | | | | |
| **FI** | **−23.0** | **4468** | **16** | **41** | **6.51** | | | | | | **4484** |
| FI-mix | −22.1 | 4461 | 20 | 20 | 1.04 | | | | | | **−23.8** |
| | | pmC | | | | | pmC | | | | |
| FJ11 | −31.8 | 111.24 | 0.39 | 0.20 | 0.27 | FJ1 | 111.02 | 0.27 | 0.20 | 0.53 | |
| FJ12 | −30.7 | 110.80 | 0.39 | 0.72 | 3.48 | | | | | | |
| FJ31 | −28.3 | 111.80 | 0.39 | 0.47 | 1.48 | FJ3 | 111.67 | 0.27 | 0.12 | 0.19 | |
| FJ32 | −28.2 | 111.54 | 0.39 | 0.18 | 0.22 | | | | | | |
| **FJ** | **−29.8** | **111.34** | **0.19** | **0.19** | **0.99** | | | | | | **110.84** |
| FJ-mix | −30.5 | 111.95 | 0.19 | 0.29 | 2.30 | | | | | | **−28.9** |

In columns with the heading "error", the uncertainties based counting statistics, standard normalization, background, and blank correction are given. In columns with the heading "$\sigma$ ", the external estimates of the uncertainty of mean values are given.

samples of the same material are more homogeneous and we obtain a reduced $\chi^2$-value of 1.2 at a precision level of 15 yrs. This indicates that an additional external uncertainty within the measurement procedure is unlikely.

Based on these results, we can summarize the system performance as follows: For individually measured cathodes we are able to reach an uncertainty level of less than 5‰. By using two cathodes of the same material, we are able to approach the 3‰ level. There are good reasons to anticipate that with a higher number of independent measurements, statistically consistent isotope ratios can be obtained at a level of 2‰ or less. However, these uncertainties cannot be directly translated into age uncertainties of the material analyzed. There are several other uncertainty components such as the possible variabilities in the sample preparation process, blank value assessment, and uncertainties of background correction which will need careful study. In any case, these are first results of a new instrument and further experiments are needed to evaluate the ultimate performance of the system.

## 4. Conclusions and outlook

The new MICADAS system is a next step in the direction to simplify AMS measurements, to reduce instrument size, to apply new technologies in AMS, and to contribute to a broader applicability of AMS technique. It is the most compact AMS system ever built which has full radiocarbon dating capability for natural samples. In contrast to other approaches [9], we carry on with the tandem AMS system. This makes possible a very compact design of the instrument and avoids open high voltage platforms. In combination with our ion source, which also confines all high voltage potentials, we have a system that can be easily operated within a common laboratory environment. The ion optics of the system makes the system easy to tune. Good beam settings are already achieved using basic setup parameters downloaded from a database. Only a few elements need to be optimized to achieve suitable measurement conditions. Once such conditions have been reached, unattended multi-day measurement campaigns can be performed.

While these performance tests clearly demonstrate the capability for high quality radiocarbon dating measurements, the interfering molecular break-up products are a source of background which, under unfavorable conditions, may limit the ultimate system performance. Here, future developments, e.g. in connection with particle identification, sample preparation procedures, and modifications of the stripper gas canal, will help to overcome this restriction.

The simple concept of the instrument makes it attractive to applications other than radiocarbon dating. In particular, the fast-growing biomedical research field which uses radiocarbon may benefit. In general, the system can be modified to reach the demands of a high throughput instrument for radiocarbon measurements at a modest uncertainty level. Those measurements would not require $\delta^{13}C$ analysis and the measurement procedure could be further simplified. We have performed initial tests and can demonstrate that $^{14}C/^{12}C$ measurements at an uncertainty level of better than 1% can be made if the extracted $^{12}C^-$ current from the source is used to normalize the detected $^{14}C$ counts. Following this idea, one could build an even smaller dedicated AMS system for biomedical applications.

## Acknowledgement

Special thanks go to I. Hajdas and S. Szidat who provided graphite samples. We are grateful to J. Thut who designed the ion source, to M. Ruff and L. Wacker who are in charge of gas ion source development and to Arnold Müller who helped to optimize detector performance. We acknowledge the special effort of the referee to improve the readability of the manuscript. Swiss National Science Foundation funds a part of the work. PSI and ETH Zürich jointly support the Zürich AMS facilities.

## References

[1] H.-A. Synal, S. Jacob, M. Suter, Nucl. Instr. and Meth. B 172 (2000) 1.
[2] H.-A. Synal, M. Döbeli, S. Jacob, M. Stocker, M. Suter, Nucl. Instr. and Meth. B 223&224 (2004) 339.
[3] M. Suter, R. Balzer, G. Bonani, W. Wölfli, Nucl. Instr. and Meth. B 5 (2) (1984) 204.
[4] H.-A. Synal, S. Jacob, M. Suter, Nucl. Instr. and Meth. B 161–163 (2000) 29.
[5] P. Sigmund, K.H. Winterbon, Nucl. Instr. and Meth. B 119 (1974) 541.
[6] M. Döbeli, C. Kottler, M. Stocker, S. Weinmann, H.-A. Synal, M. Grajcar, M. Suter, Nucl. Instr. and Meth. B 219&220 (2004) 415.
[7] S. Szidat, T.M. Jenk, H.W. Gäggeler, H.-A. Synal, I. Hajdas, G. Bonani, M. Saurer, Nucl. Instr. and Meth. B 223&224 (2004) 829.
[8] M.E. Scott et al., Radiocarbon 45 (2) (2003) 285.
[9] J.B. Schroeder, T.M. Hauser, G.M. Klody, G.A. Norton, Radiocarbon 46 (1) (2004) 1.